Bulletin of Mathematical Biology (2007) 69: 1341–1354
DOI 10.1007/s11538-006-9162-0

ORIGINAL ARTICLE

A New Method for Calculating Net Reproductive Rate from Graph Reduction with Applications to the Control of Invasive Species

T. de-Camino-Beck[a,*], M. A. Lewis[a,b]

[a] *Centre for Mathematical Biology and Department of Biological Sciences, University of Alberta, Edmonton, Alberta, Canada T6G 2E9*
[b] *Centre for Mathematical Biology and Department of Mathematical and Statistical Sciences, University of Alberta, Edmonton, Alberta, Canada T6G 2G1*

Received: 24 March 2006 / Accepted: 6 September 2006 / Published online: 15 February 2007

Abstract Matrix models are widely used for demographic analysis of age and stage structured biological populations. Dynamic properties of the model can be summarized by the net reproductive rate R_0. In this paper, we introduce a new method to calculate and analyze the net reproductive rate directly from the life cycle graph of the matrix. We show, with examples, how our method of analysis of R_0 can be used in the design of strategies for controlling invasive species.

Keywords Matrix models · Net reproductive rate · Invasion · Biological control

1. Introduction

Matrix models are widely used for demographic analysis of age and stage structured population dynamics. Population dynamics of stage structured matrix models can be analyzed by calculating the population growth rate λ, the dominant eigenvalue of the projection matrix, and the net reproductive rate R_0, the mean number of offspring per individual over its lifetime (Caswell, 2001). Here $\lambda = 1$ if and only if $R_0 = 1$. The population grows when λ or R_0 is greater than 1 and shrinks when λ or R_0 is less than 1.

One method for calculating the characteristic equation, and hence the population growth rate λ, for a stage structured model, is directly from the graph representation of a matrix model, known as the life cycle graph. In this approach, a Z-transform is applied to the graph in order to use graph reduction rules and Mason's formula to compute the characteristic equation and corresponding eigenvalues and eigenvectors (Werner and Caswell, 1977; Caswell, 1982a, 1984). Graph

*Corresponding author.
E-mail address: tomasd@math.ualberta.ca (T. de-Camino-Beck)

reduction is used to simplify matrix operations that can be tedious on large and complex matrices. Although these procedures have been well described for calculating λ (e.g Caswell, 2001), no procedure has been developed using this technique to calculate R_0.

Matrix models describe the life cycle of an organism and its effects on population change over time. For matrix population models elasticity/sensitivity analysis of the population growth rate λ, can establish events in the life cycle of the organism, when perturbed, have the most impact on population growth (Caswell, 2001). Hence, those events should be the target of biocontrol efforts (e.g. Shea and Kelly, 1998; Krivan and Havelka, 2000; Parker, 2000). The net reproductive rate R_0 can also be used to determine population growth.

The net reproductive rate has been used as persistence parameter in epidemiological literature (van den Driessche and Watmough, 2002). The biological relevance of the net reproductive rate R_0 in matrix models is widely known (see Caswell, 2001). However, this quantity has rarely been used in the analysis of population control and persistence.

In this paper, we introduce a new method to calculate the net reproductive rate directly from the life cycle graph. As far as we are aware, no such method has been proposed previously. We then show how this method can be applied, with some literature examples, to analyze the control of invading organisms. We also suggest that the net reproductive rate in matrix population models can be use to study the control of invading organisms.

1.1. Matrix models and life cycle graphs

An age or stage structured matrix model is defined as $\mathbf{n}_{t+1} = \mathbf{A}\mathbf{n}_t$, where $\mathbf{n}_t$ is a vector of ages/stages at time t and $\mathbf{A}$ is a nonnegative irreducible matrix, describing transitions from one age/stage to another one (Caswell, 2001). Matrix models can be represented by a life cycle graph, where each age/stage is represented as a node in the graph, and transitions are arcs (directed edges) from node to node. More formally, for an $n \times n$ transition matrix $\mathbf{A} = [a_{ij}]$, the associated graph $G_\mathbf{A}$ is a weighted, directed graph, whose nodes are $V = \{1, \ldots, n\}$, such that if $a_{ij} \neq 0$ in $\mathbf{A}$, there is an *arc* from j to i with weight a_{ij} in $G_\mathbf{A}$, for $i, j = 1, \ldots, n$. As an example, a matrix and its corresponding graph is shown in Fig. 1(A).

For a graph $G_\mathbf{A}$, a *path* is a sequence of arcs from one node to another. When the starting and ending nodes of a path are the same, the path is a *loop* (including a self loop at node i if $a_{ii} \neq 0$). Two paths are *disjoint* when they have no nodes in common.

1.2. Population growth λ and net reproductive rate R_0

Typical stage structured matrix models have an additional property. The transition matrix $\mathbf{A}$ is primitive. In other words, there exists a positive power of $\mathbf{A}$ whose entries are component-wise positive. For a nonnegative primitive matrix $\mathbf{A}$ the *Perron-Frobenius* theorem ensures that there is a positive and simple dominant eigenvalue λ (Horn and Johnson, 1985). This dominant eigenvalue, or population growth rate, can then be used as a parameter to establish the growth rate of the

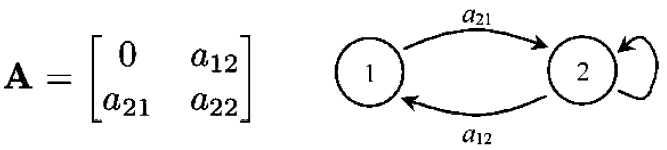

(a) Projection matrix

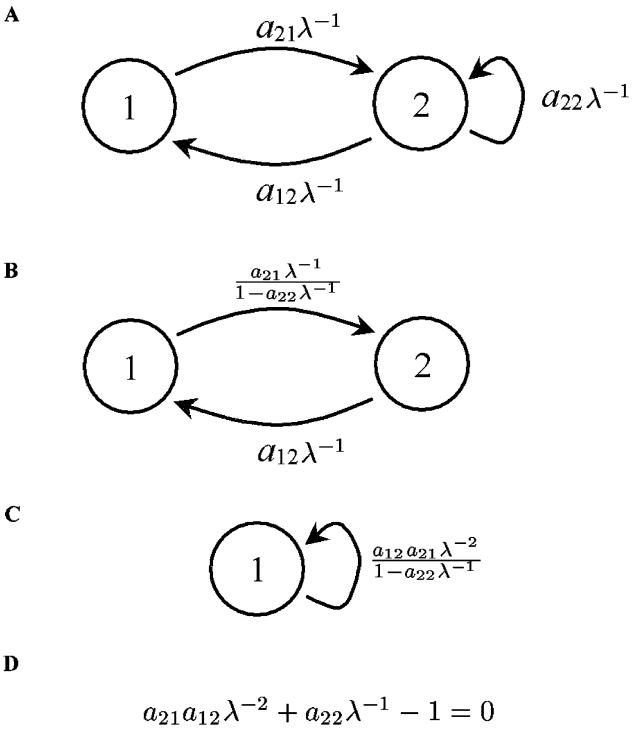

(b) Life cycle graph

Fig. 1 **A** A simple 2 node graph. **B** The z-transformed graph $\mathcal{G}_{\mathbf{A}}(\lambda)$. **C** Self loop of node 2 is eliminated using rule A of Fig. 2. **D** Node 2 is eliminated using rule E of Fig. 2. **E** Characteristic equation is calculated from Eq. (2) applied to the single-node graph given in D: $1 - L^{(1)} = 0$, where $L^{(1)} = \frac{a_{12}a_{21}\lambda^{-2}}{1-a_{22}\lambda^{-1}}$.

system described by the matrix. For matrix **A**, when $\lambda < 1$ the extinction steady state is stable, when $\lambda = 1$ the population is neutrally stable and when $\lambda > 1$ the population grows (Caswell, 2001).

To calculate R_0, the transition matrix is decomposed as $\mathbf{A} = \mathbf{T} + \mathbf{F}$, where $\mathbf{T} = [\tau_{ij}]$ (with $\tau_{ij} \in [0, 1]$ and $\sum_j \tau_{ij} \leq 1$) contains the survivorship transitions and $\mathbf{F} = [f_{ij}]$ (with $f_{ij} \geq 0$) the fecundities. Each entry in **T** describes the probability of

an individual in stage j surviving to stage i in a single time step. Since individuals in a population eventually die, it is further assumed that $\rho(\mathbf{T}) < 1$ (Li and Schneider, 2002). Once the transition and fecundity matrices are given, $\mathbf{A}$ is uniquely determined. However, decomposition of $\mathbf{A}$ into transition and fecundity matrices is not unique until information regarding the survivorship and reproduction components of each entry a_{ij} is given. This information is readily available as it is the buildings blocks of the stage-structured model. This decomposition allows for the calculation of the net reproductive rate, R_0, defined mathematically as

$$R_0 = \rho(\mathbf{F}(\mathbf{I} - \mathbf{T})^{-1}), \tag{1}$$

where $\mathbf{I}$ is the identity matrix and ρ denotes the spectral radius of the matrix $\mathbf{F}(\mathbf{I} - \mathbf{T})^{-1}$, referred to as the next generation matrix (Li and Schneider, 2002). R_0 is the strictly positive dominant eigenvalue of the matrix $\mathbf{F}(\mathbf{I} - \mathbf{T})^{-1}$ (Appendix A). It has been shown (Cushing and Zhou, 1994; Li and Schneider, 2002) that when $R_0 < 1$, the extinction state is stable, when $R_0 = 1$, the extinction state is neutrally stable and when $R_0 > 1$ the population grows. In other words, $\lambda > 1 \iff R_0 > 1$, where λ is the dominant eigenvalue of matrix $\mathbf{A}$.

2. Graph reduction of matrix models and net reproductive rate

We now introduce our new approach to calculating R_0 directly from a graph, without the need for matrix calculations. First, we review an establish graph-based method for the calculation of the characteristic polynomial for a matrix, and then we show, in the following section, the related procedure that can be used to calculate R_0.

2.1. Established graph-based method for calculating the characteristic polynomial

To compute the dominant eigenvalue λ or any other eigenvalue from the graph $G_{\mathbf{A}}$, Caswell's formula (Caswell, 1982b) for the characteristic equation of the z-transformed graph, denoted $\mathcal{G}_{\mathbf{A}}$, can be used. A z-transformed graph $\mathcal{G}_{\mathbf{A}}(\lambda)$ is defined as the graph obtained by replacing entries a_{ij} in $G_{\mathbf{A}}$ with $a_{ij}\lambda^{-1}$ (Caswell, 2001). Hence, for a population matrix $\mathbf{A}$, the characteristic equation, denoted $P(\mathcal{G}_{\mathbf{A}}(\lambda)) = 0$, yields n possible values for λ, the largest of which is the population growth rate λ and the remaining $n - 1$ values are additional smaller eigenvalues. The characteristic polynomial is defined as $P(\mathcal{G}_{\mathbf{A}}(\lambda)) = \det(\mathbf{A}\lambda^{-1} - \mathbf{I})$. If $\lambda = 1$, then $P(\mathcal{G}_{\mathbf{A}}(1)) = \det(\mathbf{A} - \mathbf{I})$. The formula for the characteristic equation, due to Hubbell and Werner (1979) and Caswell (1982b), is given by

$$P(\mathcal{G}_{\mathbf{A}}(\lambda)) = 1 - \sum_{i} L^{(i)} + \sum_{i,j}^{*} L^{(i)}L^{(j)} - \sum_{i,j,k}^{*} L^{(i)}L^{(j)}L^{(k)} + \cdots = 0, \tag{2}$$

where $L^{(i)}$ is the product of arc coefficients in the ith loop in the graph $\mathcal{G}_{\mathbf{A}}(\lambda)$, and the asterisk indicates that the sum is taken over the product of all pairs,

triplets, . . . , $n-$tuples of disjoint loops. See Mason and Zimmermann (1960) and Chen (1976) for a detailed derivation of the formula and Caswell (2001) for applications to life cycle graphs.

By way of example consider the life cycle graph shown in Fig. 1. From the graph shown in Fig. 1A, there are two loops, $L^{(1)} = a_{22}\lambda^{-1}$ and $L^{(2)} = a_{12}a_{21}\lambda^{-2}$. Applying Eq. (2), we get $P(\mathcal{G}_{\mathbf{A}}(\lambda)) = 1 - (a_{22}\lambda^{-1} + a_{21}a_{12}\lambda^{-2}) = 0$.

For a complicated life cycle graph calculation using Eq. (2) can be onerous. However, the same result can be obtained via graph reduction, a procedure that allows for the elimination of paths and nodes from a graph. Since a graph is a representation of a system of linear equations, graph reduction is equivalent to elimination of variables (nodes) by back-substitution. The application of graph reduction simplifies the calculation of Eq. (2). A graph can be reduced using the rules shown in Fig. 2. An important property of graph reduction is that the dynamic properties of the system remain invariant under graph reduction (Caswell, 2001), that is, the characteristic equation remains invariant (Chen, 1976; Lewis, 1977). As shown in Fig. 1, a graph can be reduced completely to one node to obtain the characteristic

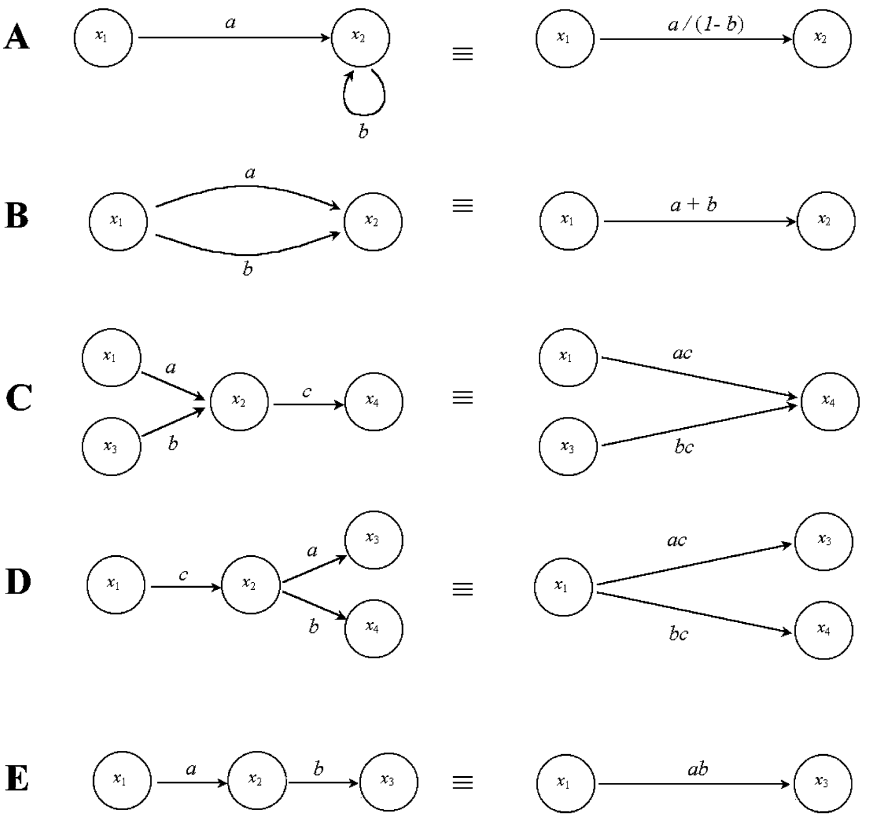

Fig. 2 Mason equivalence rules for graph reduction (modified from Caswell, 2001). **A** Self loop elimination. **B** Parallel paths elimination. **C, D** and **E** Elimination of node x_2.

equation directly. From the previous example (Fig. 1), using graph reduction we obtain the same result (Fig. 1E).

2.2. *Calculating R_0 from the graph*

As mentioned earlier, given a projection matrix, the net reproductive rate can be calculated using Eq. (1). To connect the calculation of R_0 with graph reduction methods we first observe that, the net reproductive rate is determined uniquely by

$$\rho(R_0\mathbf{T} + \mathbf{F}) = R_0, \tag{3}$$

where ρ denotes the spectral radius. For detailed derivation of Eq. (3), see Appendix A.

Now, given Eq. (3), we can use the *z-transform* of the matrix $\mathbf{B} = R_0\mathbf{T} + \mathbf{F}$, to calculate using Eq. (2), the characteristic polynomial of $\mathbf{B}$, $P(\mathcal{G}_{\mathbf{B}}(R_0))$. Note that $\mathcal{G}_{\mathbf{B}}(R_0)$ can be related to the graph of $\mathbf{A}$, $G_{\mathbf{A}}$, as follows: each entry $a_{ij} = t_{ij} + f_{ij}$ in $G_{\mathbf{A}}$ is replaced by $b_{ij}R_0^{-1} = (R_0 t_{ij} + f)R_0^{-1} = t_{ij} + fR_0^{-1}$. In other words, $\mathcal{G}_{\mathbf{B}}(R_0)$ is found by multiplying the fecundity transitions in $G_{\mathbf{A}}$ by R_0^{-1}.

As we did previously, we can again apply Mason's rules for graph reduction now to solve $P(\mathcal{G}_{\mathbf{B}}(R_0)) = 0$ for R_0. According to Eq. (3), R_0 is the dominant eigenvalue of $\mathbf{B}$, and hence satisfies $P(\mathcal{G}_{\mathbf{B}}(R_0)) = 0$.

As an example, consider a case where $\mathbf{T}$ and $\mathbf{F}$ are as shown in Fig. 3**a**. Figure 3 shows the graph reduction procedure to obtain the characteristic equation for this example. Note that the rank of $\mathbf{F}$ is one and therefore the polynomial $P(\mathcal{G}_{\mathbf{B}})$ is a polynomial of degree 1; hence, there is only one possible value for R_0.

Suppose that $\tilde{\mathcal{G}}_{\mathbf{B}}$ is the graph obtained from applying Mason's rules to $\mathcal{G}_{\mathbf{B}}$. We can always apply Eq. (2) to obtain $P(\tilde{\mathcal{G}}_{\mathbf{B}})$, and then solve for R_0, or we can continue with reduction until there is one node left. In either case, R_0 remains invariant, but the graph reduction method its easier to apply and the result yields a simplified equation.

In most life cycles, expressions for R_0 are given explicitly, vegetative reproduction (or clonal reproduction) can lead to more complex reduced graphs, such as the one shown in Fig. 4. Note that all the fecundity transitions in Fig. 4A are multiplied by R_0^{-1}, that in the reduced graph (Fig. 4C) fecundity paths contain the term R_0^{-1}, and that these fecundity loops are not disjoint. To calculate R_0, we apply formula (1) on the matrix corresponding to the remaining reduced graph to calculate R_0. This type of graph can occur when there is vegetative reproduction (see for example Dinnetz and Nilsson, 2002), and fecundity pathways in the life cycle graph that can reproduce independently from other pathways.

In summary, given the matrix $\mathbf{B} = R_0\mathbf{T} + \mathbf{F}$, and the corresponding graph $\mathcal{G}_{\mathbf{B}}$, the graph reduction algorithm to calculate R_0 can be applied as follows: (1) Eliminate survivorship self-loops from $\mathcal{G}_{\mathbf{B}}$, (2) Reduce the graph until only nodes with fecundity self-loops are left, (3) If only one node is left, then eliminate the final node and the result will be R_0; otherwise solve the polynomial that comes from applying Eq. (1) to the reduced graph.

$$\mathbf{T} = \begin{bmatrix} a_{11} & 0 & 0 \\ a_{21} & 0 & 0 \\ a_{31} & a_{32} & 0 \end{bmatrix} \qquad \mathbf{F} = \begin{bmatrix} 0 & 0 & a_{13} \\ 0 & 0 & a_{23} \\ 0 & 0 & a_{33} \end{bmatrix}$$

(a) Projection matrix

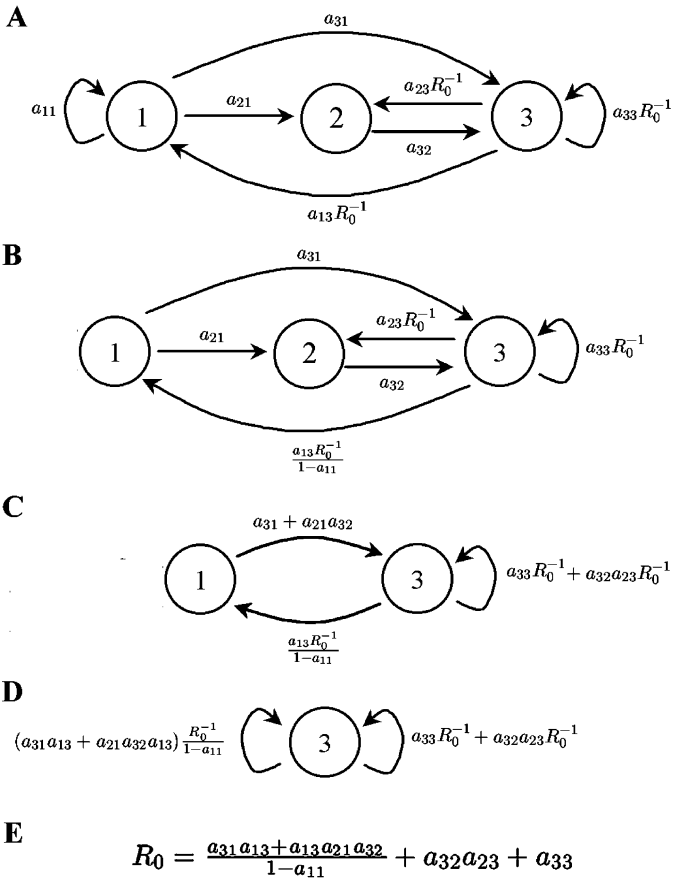

(b) Life cycle graph reduction

Fig. 3 **a** An example of a transition and fecundity matrix.**b** Graph reduction procedure. **A** The full transformed graph (with associated matrices **a**). **B** Eliminating self-loop in node 1. **C** Eliminating node 2. **D** Eliminating node 1. **E** Eliminating node 3 and solving for R_0.

3. Applications

A *fecundity pathway* is a loop of any length where there is only one fecundity transition involved. As we will demonstrate in this section, the graph reduction method provides an expression for R_0 as a sum of contributions from the different

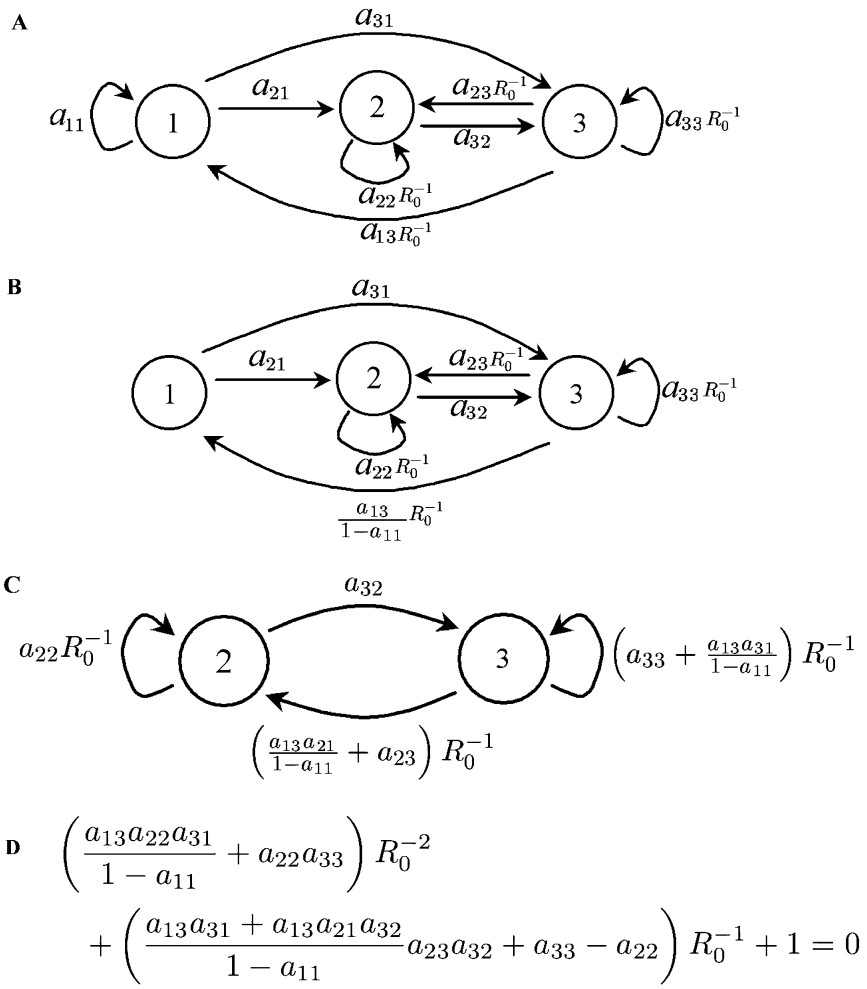

Fig. 4 Hypothetical life cycle graph with vegetative reproduction. This graph is the same as Fig. 3A, except an additional self loop is added in node 2. **A**. full graph, **B**. Elimination of self loop in node 1, **C**. Elimination of node 1, **D**. R_0 equation.

possible fecundity pathways. Biologically, it is a sequence of steps in the life cycle that lead to the production of new individuals.

3.1. Scentless chamomile (Matricaria perforata)

Scentless chamomile is an introduced annual, biennial or short-lived perennial plant that has become a widely distributed weed in cultivated areas in North America (Hinz, 1996; Hinz and McClay, 2000). In Hinz (1996), a stage-structure model is developed, and transition values are compared between different disturbance treatments (soil disturbance and herbivory). The full life cycle is shown in Fig. 3A.

Hinz (1996) showed, using elasticity matrices, that, in general, transition from rosettes to flowering plants a_{32} and fecundity transitions a_{23} and a_{33} contributed the most to population growth and would therefore be the most effective transitions to control.

We calculate R_0 by applying the graph reduction procedure (Fig. 3),

$$R_0 = \underbrace{\frac{a_{31}a_{13} + a_{13}a_{21}a_{32}}{1 - a_{11}}}_{\text{new flowers from seeds}} + \underbrace{a_{32}a_{23}}_{\text{new flowers from rosettes}} + \underbrace{a_{33}}_{\text{new flowers from flowers}} \tag{4}$$

The fecundity pathways are given below each term in the equation. Examination of R_0 gives additional insight into possible control strategies. The fecundity transitions are a_{13}, a_{23}, a_{33}. Note that, if transition a_{33} is larger than one, $R_0 > 1$ regardless of the contributions of other transitions, and population increase will occur. Similarly if the loop $a_{32}a_{23} > 1$ then the population will increase regardless of the other fecundity pathways. This is consistent with Hinz's results (Hinz, 1996), which based on numerical estimates of matrix transition entries, showed elasticity matrices where a_{33}, a_{32} and a_{23} affect population growth the most.

Our analyses suggests, that any control strategy must focus on reducing fecundity below a critical level. However, this action alone would not ensure successful control. For example, as seed bank survival a_{11} approaches 1, the term $(1 - a_{11})^{-1}$ becomes large and the population will increase. Hinz (1996) found that transitions a_{13}, a_{31} and a_{21} to be of minor importance. However, it can be seen from the R_0 equation that this situation would probably change as a_{11} increases. With this example, we have shown how the analysis of fecundity pathways using R_0 can complement the design of effective control strategies.

3.2. Nodding thistle (Carduus nutans)

Shea and Kelly (1998) derived a matrix model to study the control of nodding thistle (*Carduus nutans*), a weed that causes economic damage to grazing lands in New Zealand. The authors described the life cycle of *C. nutans* by the graph in Fig. 5A. They concluded using elasticity analysis that seed to seedling and small-plants to seeds transitions contribute the most to λ (g_{21} and r_{12} in the graph). Their numerical results, based on numerical estimates of matrix transitions, indicate that seed losses of 69% are required to reduce the weed populations. A 30%–40% reduction in seed production has been unsuccessful in New Zealand, but successful in North America, which contradicts the numerical results and suggests regional differences. Their general conclusion was that, to control *C. nutans*, a large reduction in seed bank and suppression of germination is needed. For comparison, using graph reduction we obtained the 2 node graph in Fig. 5C, and further elimination yields:

$$R_0 = r_{22} + g_{42}r_{24} + g_{32}r_{23} + g_{32}g_{43}r_{24} + \frac{g_{21}r_{12} + g_{21}g_{32}r_{13} + g_{21}g_{42}r_{14} + g_{32}g_{43}g_{21}r_{14}}{1 - s_{11}}. \tag{5}$$

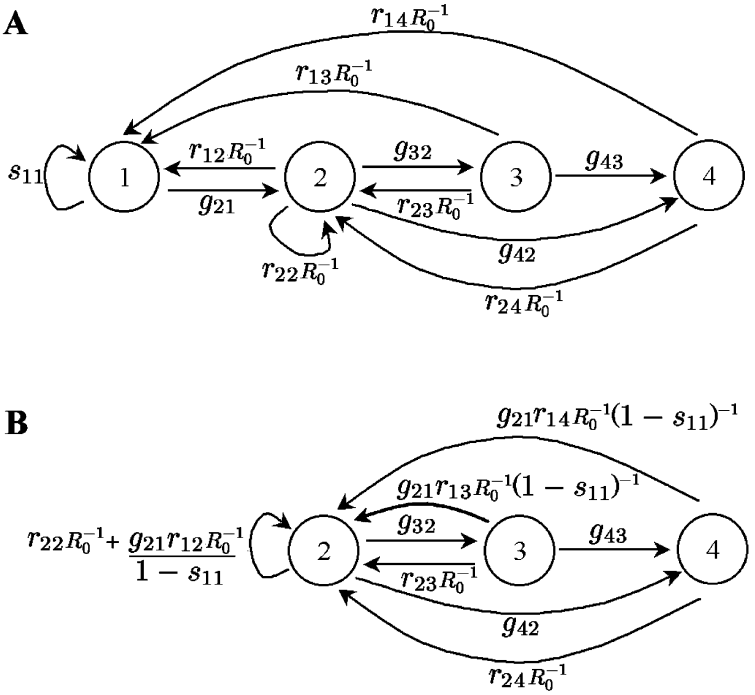

Fig. 5 Nodding thistle life cycle graph as described by Shea and Kelly (1998). Node 1, seed bank; nodes 2, 3 and 4, small, medium, and large plants. Reproductive transitions are labelled r_{ij} coming out of three nodes (2, 3, 4). **A** Full transformed graph. **B** Elimination of node 1. **C** Elimination of node 4. **D** Resulting net reproductive rate.

It is evident from R_0 that if only survivorship g_{21} is reduced by control, but small plant fecundities (r_{12} and r_{22}) are not, then since $r_{22} > 1$ the system is unstable ($R_0 > 1$). As with the previous example, as s_{11} approaches 1, the term $(1 - s_{11})^{-1}$ becomes large, driving R_0 above one. This is consistent with Shea and Kelly (1998), with g_{21} included in all pathways involving a_{11}, but it provides a more general result because we do not require numerical analysis to get to this result.

Shea and Kelly (1998) suggest that grazing could contribute substantially to thistle control. We extend the graph reduction procedure to calculate R_0 to explore the combined effects of biocontrol and grazing. To simplify analysis further, we focus on the reproductive pathways, denoting $P_{1,2,\ldots,n}$ as a reproductive path that goes through nodes $1, 2, \ldots, n$. Equation (5) can be rewritten as

$$R_0 = \left[P_2 + P_{2,3} + P_{2,4} + P_{2,3,4} + \left(\frac{P_{1,2} + P_{1,2,3} + P_{1,2,4} + P_{1,2,3,4}}{1 - s_{11}} \right) \right] \tag{6}$$

where $P_2 = r_{22}$, $P_{2,3} = g_{32}r_{23}$, $P_{2,4} = g_{42}r_{24}$, $P_{2,3,4} = g_{32}g_{43}r_{24}$, $P_{1,2} = g_{21}r_{12}$, $P_{1,2,3} = g_{21}g_{32}r_{13}$, $P_{1,2,4} = g_{21}g_{42}r_{14}$ and $P_{1,2,3,4} = g_{32}g_{43}g_{21}r_{14}$.

Suppose a biocontrol agent is used to control fecundity of reproductive plants (transitions into node 1). The reduction in seed production is represented by scaling variable u_1. The level of grazing, which reduces germination and affects transition g_{21} , is represented by u_2, where $0 \leq u_i \leq 1$ is the proportional reduction in pathways. Note that all the fecundity paths go through node 2 or node 1. So, we can rewrite $P_{i\cdot}^k$ as the pathways of length k that start and end in node i. The R_0 equation can thus be rewritten as

$$R_0 = (1 - u_1) \sum_k \frac{P_{1\cdot}^k}{1 - s_{11}} + (1 - u_2) \sum_k P_{2\cdot}^k \tag{7}$$

If $u_1 = 0$, meaning no effort is applied to control germination (i.e. the only control of the path from node 1 to 2 is grazing), then we need a larger proportional reduction in grazing to control the system. Note that in this case control u_2 is chosen based on the number of pathways where transition from 1, 2 is involved. This method confirms analytically the suggestion of Shea and Kelly (1998) that grazing could complement biological control.

4. Conclusion

While it is possible to calculate the net reproductive rate R_0 directly from Eq. (1) using matrix algebra, the resulting expression is no longer easily interpreted in terms of fecundity pathways, unless extensive rearrangement is undertaken (Appendix B).

Because of their dynamical properties, λ and R_0 are demographic parameters by which optimization can be applied to design a control strategy for unwanted species. As we show here, with the new method given in this paper, it is straightforward to obtain an analytical formula for R_0 using graph reduction methods. As

far as we are aware, this method is entirely new and has not been used to calculate R_0 previously.

It is our understanding of the fecundity pathways in R_0 that allows us to derive and analyze control strategies for invasive species. As shown in the examples, when the method is used, the expression for R_0 is given as a sum of contributions from different fecundity pathways (see for example Eq. (4)) The examples show that some analysis of the R_0 equation can aid in biocontrol target selection and more generally in the design of control and conservation strategies. In some cases perturbations in the transition matrix that decrease R_0 may increase λ and vice versa (Caswell, 2001). Nonetheless since $R_0 < 1$ implies $\lambda < 1$, a control strategy that guarantees $R_0 < 1$ for biocontrol, or $R_0 > 1$ for conservation, can be useful in the first stages of planning and can be refined as more data are obtained. Analogous to compartmental models of disease transmission, where the basic reproductive number determines a disease-free equilibrium (van den Driessche and Watmough, 2002), in matrix population models of invading organisms, R_0 determines persistence of the invader, and this quantity can be used to determine control strategies. In this way, the use of R_0 is a useful alternative to numerical analysis of λ for designing a general control strategy framework that can be customized to accommodate different parameter values in different regions.

Acknowledgements

We thank Pauline van den Driessche, Alex Potapov, Marjorie Wonham and Erik Noonburg for helpful discussion and comments on the manuscript. We also thank Hal Caswell and anonymous reviewers for valuable comments on the manuscript. T.de-C.-B. was supported by MITACS, and a University of Alberta Studentship. M.A.L. gratefully acknowledges support from Natural Sciences and Engineering Research Council of Canada Discovery and Collaborative Research Opportunities Grants and a Canada Research Chair.

Appendix: A Derivation of the R_0 equation

Our goal is to show how to derive equation $R_0 = \rho(R_0\mathbf{T} + \mathbf{F})$. The projection matrix $\mathbf{A} = \mathbf{T} + \mathbf{F}$, can be decomposed into survivorship transitions $\mathbf{T}$ and fecundity $\mathbf{F}$. The survivorship matrix contains the probability of stage transitions $\mathbf{T} = [\tau_{ij}]$ with $0 \leq \tau_{ij} \leq 1$, $\rho(\mathbf{T}) < 1$, and $\sum_j \tau_{ij} \leq 1$. The fecundity matrix $\mathbf{F}$ has entries $f_{ij} \geq 0$. We know that $(\mathbf{I} - \mathbf{T})^{-1}$ is nonnegative, because $\mathbf{T}$ is nonnegative, $\rho(\mathbf{T}) < 1$ and $\lim_{k\to\infty} \mathbf{T}^k = 0$ means $(\mathbf{I} - \mathbf{T})^{-1} = \mathbf{I} + \mathbf{T} + \mathbf{T}^2 + \ldots$ is nonnegative. By definition $\mathbf{F} \geq 0$. Hence $\mathbf{F}(\mathbf{I} - \mathbf{T})^{-1}$ is also nonnegative. Let λ_ρ be the eigenvalue of $\mathbf{F}(\mathbf{I} - \mathbf{T})^{-1}$ with $|\lambda_\rho| = R_0$ (Eq. (1)). Since $\mathbf{F}(\mathbf{I} - \mathbf{T})^{-1}$ is nonnegative, there is a nonnegative left eigenvector (Perron vector) $\mathbf{u}^T$ corresponding to λ_ρ that satisfies $\mathbf{u}^T\mathbf{F}(\mathbf{I} - \mathbf{T})^{-1} = \lambda_\rho\mathbf{u}^T$. The eigenvalue λ_ρ is real and positive, hence $\lambda_\rho = R_0$ is the dominant eigenvalue of $\mathbf{F}(\mathbf{I} - \mathbf{T})^{-1}$. Now, $\mathbf{u}^T\mathbf{F} = R_0\mathbf{u}^T(\mathbf{I} - \mathbf{T}) = R_0\mathbf{u}^T\mathbf{I} - R_0\mathbf{u}^T\mathbf{T}$. Therefore,

$$\mathbf{u}^T(\mathbf{F} + R_0\mathbf{T}) = \mathbf{u}^T\mathbf{F} + R_0\mathbf{u}^T\mathbf{T} = R_0\mathbf{u}^T \tag{A.1}$$

The matrix $\mathbf{A} = \mathbf{T} + \mathbf{F}$ is irreducible, hence $G_{\mathbf{A}}$ is strongly connected (see Horn and Johnson, 1985). Since $R_0 > 0$, then the graph corresponding to $R_0\mathbf{T} + \mathbf{F}$ is also strongly connected, hence $R_0\mathbf{T} + \mathbf{F}$ is irreducible. By Theorem 2.1b in Li and Schneider (2002), it follows that R_0 is the unique dominant eigenvalue. From Eq. (A.1) we can write the formula for R_0 as, $R_0 = \rho(R_0\mathbf{T} + \mathbf{F})$. A similar argument is used to prove Theorem 3.1 in Li and Schneider (2002).

B Algebraic and graph calculation of R_0

Algebraic calculation of R_0 is nontrivial. First the inverse of $\mathbf{I} - \mathbf{T}$ must be computed and then the eigenvalues of $\mathbf{F}(\mathbf{I} - \mathbf{T})^{-1}$ must be solved. Usually this is done using a symbolic programming language like *Maple* or *Mathematica*. As an example, consider the transition and fecundity matrices for thistle,

$$\mathbf{T} = \begin{bmatrix} s_{11} & 0 & 0 & 0 \\ g_{21} & 0 & 0 & 0 \\ 0 & g_{32} & 0 & 0 \\ 0 & g_{42} & g_{43} & 0 \end{bmatrix}, \mathbf{F} = \begin{bmatrix} 0 & r_{12} & r_{13} & r_{14} \\ 0 & r_{22} & r_{23} & r_{24} \\ 0 & 0 & 0 & 0 \\ 0 & 0 & 0 & 0 \end{bmatrix} \tag{B.1}$$

In *Mathematica 5.2*, once matrices $\mathbf{T}$ and $\mathbf{F}$ are specified, R_0 is calculated using the commands,

```
Eigenvalues[F. Inverse[IdentityMatrix[n]-T]]
```
(B.2)

Asking *Mathematica 5.2* to produce a simplified solution we get as an output,

$$\begin{aligned} R_0 = \frac{1}{a_{11} - 1}[&-a_{21}r_{12} - a_{21}a_{32}r_{13} - a_{21}a_{42}r_{14} - a_{21}a_{32}a_{43}r_{14} \\ &+ a_{11}r_{22} - r_{22} + a_{11}a_{32}r_{23} - a_{32}r_{23} + a_{11}a_{42}r_{24} \\ &- a_{42}r_{24} + a_{11}a_{32}a_{43}r_{24} - a_{32}a_{43}r_{24}] \end{aligned} \tag{B.3}$$

By way of contrast, the calculation of R_0 using the graph reduction method is shown in Fig. 5. Note how terms represent fecundity pathways, pathways that start in a reproducing stage and return to that stage after passing several transitions. When reducing the graph, all these pathways are evident and operations yield a simple equation expressed in terms of fecundity pathways, compared to the computer output in Eq. (B.3).

References

Caswell, H., 1982a. Optimal life histories and the age-specific costs of reproduction. J. Theor. Biol. 98(3), 519–529.

Caswell, H., 1982b. Optimal life histories and the maximization of reproductive value—a general theorem for complex life-cycles. Ecology 63(5), 1218–1222.

Caswell, H., 1984. Optimal life histories and age-specific costs of reproduction—2 extensions. J. Theor. Biol. 107(1), 169–172.

Caswell, H., 2001. Matrix population models: construction, analysis, and interpretation, 2nd edn. Sinauer Associates.
Chen, W., 1976. Applied graph theory; graphs and electrical networks, 2nd edn. North-Holland Pub. Co.
Cushing, J., Zhou, Y., 1994. The net reproductive value and stability in matrix population models. Nat. Res. Model. 8(4), 297–333.
Dinnetz, P., Nilsson, T., 2002. Population viability analysis of *Saxifraga cotyledon*, a perennial plant with semelparous rosettes. Plant Ecol. 159(1), 61–71.
Hinz, H., 1996. Scentless chamomile, a target weed for biological control in Canada: Factors influencing seedling establishment. In: Proceedings of the IX International Symposium on Biological Control of Weeds, pp. 187–192.
Hinz, H., McClay, A., 2000. Ten years of scentless chamomile: Prospects for the biological control of a weed of cultivated land. In: Proceedings of the X International Symposium on Biological Control of Weeds, pp. 537–550.
Horn, R., Johnson, C., 1985. Matrix Analysis. Cambridge University Press.
Hubbell, S., Werner, P., 1979. Measuring the intrinsic rate of increase of populations with heterogeneous life histories. Am. Nat. 113(2), 277–293.
Krivan, V., Havelka, J., Feb 2000. Leslie model for predatory gall-midge population. Ecol. Modell. 126, 73–77.
Lewis, E., 1977. Network models in population biology. Springer-Verlag.
Li, C., Schneider, H., 2002. Applications of Perron-Frobenius theory to population dynamics. J. Math. Biol. 44(5), 450–462.
Mason, S., Zimmermann, H., 1960. Electronic circuits, signals, and systems. Wiley.
Parker, I., 2000. Invasion dynamics of *Cytisus scoparius*: a matrix model approach. Ecol. Appl. 10(3), 726–743.
Shea, K., Kelly, D., 1998. Estimating biocontrol agent impact with matrix models: *Carduus nutans* in New Zealand. Ecol. Appl. 8(3), 824–832.
van den Driessche, P., Watmough, J., Nov 2002. Reproduction numbers and sub-threshold endemic equilibria for compartmental models of disease transmission. Math. Biosci. 180, 29–48.
Werner, P., Caswell, H., 1977. Population-growth rates and age versus stage-distribution models for teasel (*Dipsacus sylvestris* Huds). Ecology 58(5), 1103–1111.